# Flexural Rigidity Characterization of Retrofitted FRP Plates

STEVEN J. MAKONIS JR.
Frank Batten School of Engineering and Technology
Old Dominion University
Norfolk, VA 23529
USA
smako001@odu.edu

STELLA B. BONDI
Frank Batten School of Engineering and Technology
Old Dominion University
Norfolk, VA 23529
USA
Phone 757-683-3775; fax 757-683-5655
sbondi@odu.edu

ZIA RAZZAQ
Frank Batten School of Engineering and Technology
Old Dominion University
Norfolk, VA 23529
USA
zrazzaq@odu.edu

*Abstract:* - Presented herein is a procedure and numerical results for flexural rigidity characterization of Fiber Reinforced Polymer (FRP) plates retrofitted with various types of fabrics. The FRP plates were retrofitted with Kevlar® 49 (Aramid), Carbon Fiber (Harness-Satin H5), and Unidirectional Carbon Fiber (T700 Aerospace Grade) fabrics, respectively. The FRP plate flexural rigidity values were calculated with a central finite-difference iterative scheme while utilizing the experimental load-deflection relations based on bending tests. The tests were performed on each plate by applying a concentrated load at the center. A fourth-order partial differential equation of plate equilibrium was adopted to estimate the plate flexural rigidities and ultimately obtain the theoretical load-deflection relations. The results were verified with Navier's solution for the same type of loading. Excellent agreement was found between the two approaches. The flexural rigidity estimation procedure can be used for more complex retrofitted plates while utilizing homogenous plate deflection equations. The FRP plates showed a significant increase in flexural rigidity, with the Aerospace Grade Carbon fiber fabric providing the most significant increase.

*Key-Words:* - FRP, Kevlar, Carbon Fiber, finite-difference, flexural rigidity, retrofitting

## 1 Introduction

Retrofitting composite plates to gain structural stiffness is of practical importance. Fiber Reinforced Polymer (FRP) composites are attractive due to an absence corrosion and magnetic interference. Such characteristics make FRP products very attractive for both civil as well as marine engineering where chemically corrosion-resistant structures are required. Although such materials have a high strength-to-weight ratio, they typically tend to have low flexural stiffness or rigidity. The main focus of the paper is on investigating the suitability of different types of composite fabrics when used for retrofitting rectangular FRP plates for the purpose of increasing the flexural rigidity.

Figure 1 shows an example of the FRP plate Pultex® 1625 series cut in four segments for simplicity in finite-difference computations.
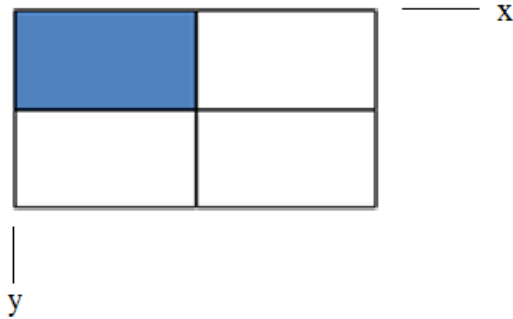
Fig. 1 – Fiber Reinforced Polymer plate

Kevlar® is the trade name for a polymer known as polyarylamide [1]. It has certain stiffening properties that could be beneficial if used correctly. Typically the material is spun into ropes or fabric sheets to be used in racing tires, bicycle tires, racing sails and body armor. When woven it becomes more suitable for mooring lines and other underwater applications. Figure 2 shows the FRP plate epoxied with Kevlar® 49 (Aramid) fabric.
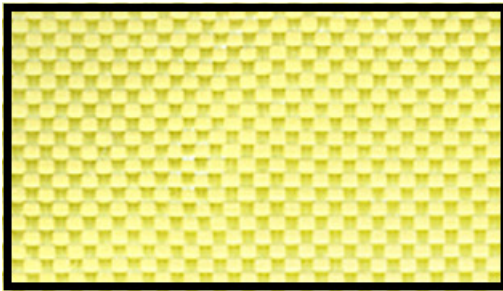


Fig. 2 - FRP plate epoxied with Kevlar® 49 (Aramid)

Carbon fiber woven fabrics are used for reinforcement when combined with either a polyester, epoxy or vinyl ester resin [2]. It can be utilized as high performance reinforcement for automotive, marine, audio and aesthetic applications [4]. Carbon fiber fabrics are becoming more known for their use in many applications due to their light weight and high strength. There are two types of carbon fiber fabrics. The first is a general biaxial anisotropic woven fabric. Figure 3 shows the FRP plate epoxied with Carbon fiber woven fabric.
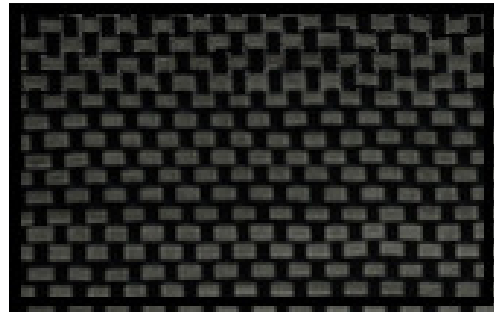


Fig. 3 - FRP plate epoxied with H5 Carbon Fiber

Another isotropic fabric is the Unidirectional Carbon Fiber-T700 Aerospace Grade fabric [2]. It is manufactured for aerospace and racing applications where maximum single-directional properties are critical. Figure 4 shows the FRP plate epoxied with Unidirectional Carbon Fiber (T700 Aerospace Grade) fabric.
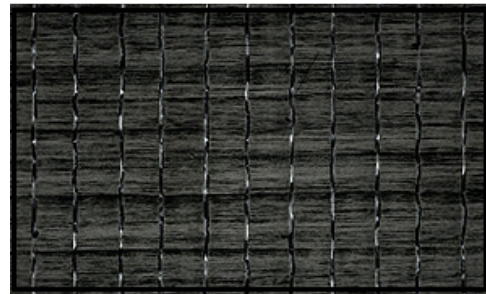


Fig. 4 - FRP plate epoxied with Unidirectional Carbon Fiber (T700 Aerospace Grade) fabric

This research report investigates the effectiveness of three types of fabrics for retrofitting FRP rectangular plates with the goal of increasing their flexural rigidity. The plate flexural rigidities are determined by an iterative use of a finite-difference solution scheme for the fourth-order partial differential equation coupled with experimentally obtained load-deformation data.

MATLAB® or matrix laboratory is a numerical computing environment and fourth-generation programming language. The software was used in the matrix manipulation of the finite-difference method for the theoretical calculations.

## 2  Literature Review

In 1939, Roy and Chakraborty [10] presented an article that dealt with assessment of impact-induced delamination in hybrid fiber reinforced plastic laminated composites.   The studies have been conducted on graphite/epoxy and Kevlar®/epoxy laminates as well as graphite/epoxy–Kevlar®/epoxy hybrid laminates to determine their responses to impact loading.  Eight-node layered solid elements have been used for finite element modeling of FRP laminates.   Newmark-method along with Hertzian contact law has been used for transient dynamic finite element analysis.  Stresses at the interfaces have been calculated using least-square formulation proposed by Hinton and Campbell.  Based on the stresses calculated, delaminations at the interfaces have been assessed using appropriate delamination criterion.  It has been observed that even though the contact force magnitude is much less in the case of Kevlar®/epoxy laminates compared to that in graphite/epoxy laminates, the number of interfaces where delamination occurs as well as the delamination extent is greater in the case of Kevlar®/epoxy laminates.  From this study it could be observed that Kevlar®/epoxy–graphite/epoxy laminate is a better choice for guarding against impact-induced failure in laminated composites.

In 2001, Rahimi and Hutchinson [11] reinforced concrete beams with bonding fiber-reinforced plastics.  The experimental work included flexural testing of 2.3-m-long concrete beams with bonded external reinforcements.  The test variables included the amount of conventional (internal) reinforcement and also the type and amount of external reinforcement.  For comparison, some of the beams were strengthened with bonded steel plates.  Theoretical analyses included 2D nonlinear finite-element modeling incorporating a "damage" material model for concrete.  In general there were reasonably good correlations between the experimental results and nonlinear finite-element models.  It is suggested that the detachment of bonded external plates from the concrete, at ultimate loads, is governed by a limiting principal stress value at the concrete/external plate interface.

In 2007, Yeh, Wang, Jang [12], analyzed the large deflections of an orthotropic rectangular clamped and simply supported thin plate.  A hybrid method which combines the finite difference method and the differential transformation method is employed to reduce the partial differential equations describing the large deflections of the orthotropic plate to a set of algebraic equations.  The simulation results indicated that significant errors are present in the numerical results obtained for the deflections of the orthotropic plate in the transient state when a step force is applied.  The magnitude of the numerical error is found to reduce, and the deflection of the orthotropic plate to converge, as the number of sub-domains considered in the solution procedure increases.  The deflection of the simply supported orthotropic plate is great than the clamped orthotropic plate.  The current modeling results confirm the applicability of the proposed hybrid method to the solution of the large deflections of a rectangular orthotropic plate.

In 2010, Kim, Yoo [13], presented a novel analytical solution for the flexural response of annular sector thin-plates.  An exact solution has been developed in the series form including trigonometric and exponential functions in the polar coordinate system for annular sector plates subjected to uniform loading.  The salient feature of the solution development includes the derivation of a closed-form solution for the fourth-order partial differential equation governing plate deflections in the polar coordinate system.  The series solution developed in this study is not only very stable but also exhibits rapid convergence.  To demonstrate the convergence and accuracy of the present method, several examples with various sector angles are selected and analyzed.  Deflections and moments of example sector plates by the proposed solution are compared with those obtained by other analytical studies and then verified by numerical values evaluated by a commercial finite element analysis program, ABAQUS.  Excellent agreements have been found between the results from the proposed analytical closed-form solution and numerical runs, there by confirming the superior nature of the proposed method over other classical analytical techniques.

The small scale comparison of multiple fabrics epoxied plates using the flexural rigidity term and with the use of the finite-difference method has not be previously published.

## 3 Problem Formulation

This research report features an experimental and theoretical flexural study of retrofitted thin rectangular plates.  The purpose of this is to investigate the elastic flexural stiffness of FRP composite plates retrofitted with Kevlar®, Carbon

fiber and Aerospace Grade Carbon fiber fabrics. The theoretical analysis additionally includes the use of the finite-difference method to iteratively compute theoretical flexural rigidity values. Figure 5 demonstrates a simply-supported rectangular plate subjected to a concentrated point load P.
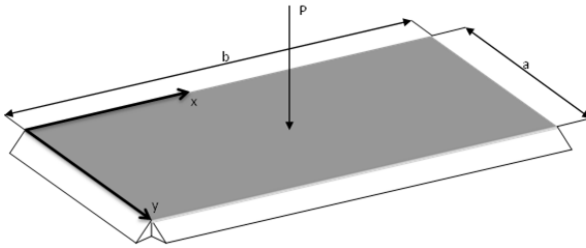


Fig. 5 - Rectangular Plate with Concentrated Load

The following issues are addressed in this research report:

1)  Can a combination of the finite-difference method and experimental load-deflection relations be used to determine plate flexural rigidity accurately? Would the outcome agree with Navier's solution?
2)  Is there a way to compare the overall stiffness of retrofitted FRP plates?
3)  Which of the three epoxied fabrics increases the stiffness of the total system the best?
4)  Can an approach be formulated to calculate equivalent material thickness of a fabric used for retrofitting an FRP plate?

# 4  Experimental Results

## 4.1 Panel Fabrication
Four FRP plates 60.96 x 121.92 cm. of Pultex® 1625 series were custom cut from the same piece of material for the purpose of this experiment [3]. The first FRP plate was the control plate, meaning that this sample will be used to compare the other specimens too. The second plate was epoxied with a single layer of Kevlar® 49. The third FRP plate was epoxied with a single layer of composite fabric called 100% carbon fiber with a weave of Harness-Satin H5. The fourth FRP plate was epoxied with

T-700 Aerospace grade fiber fabric. Since the fabrics initial design is only unidirectional, while the other fabrics are bi-directional, the final plate was epoxied with two layers perpendicular to each other. The strain gauges were installed in a predetermined position, off center in the middle of the plates; there was an initial concern that the strain gauges could develop unrealistic results due to the epoxied mounting and lamination of the fabrics.

## 4.2 Epoxy-Resin and Hardener
Epoxy comes typically as a two part system: Resin and Hardener. The epoxy used for this experiment was a clear epoxy called West Systems® 207 Epoxy Hardener that has a moderate cure rate. The hardener used was West Systems®105 Epoxy Resin. The hardener and resin used in this experiment was a 3:1 ratio. The epoxy mix was applied very thin and allowed to dry per the manufacturer's recommendations.

## 4.3 Experimental Summary of Test Results
The blank FRP plate is being used as the base control test. The results are the average values from multiple tests. The FRP plate has a deflection-to-thickness ratio of 15.8%. As the different fabrics were tested the results show a lowered ratio signifying the increase in stiffness and a more capable retrofitting material. The FRP with Kevlar® coating had a ratio of 12.5%, the Carbon fiber had a ratio of 13.7% and the Aerospace Carbon fiber had a ratio of 9.2%. The Aerospace Carbon fiber increased the stiffness dramatically in comparison to the FRP. The Carbon fiber produced better results than Kevlar® experimentally.

# 5  Theoretical Equations

## 5.1 Navier's Solution
Using Navier's solution for the maximum deflection at the center of the plate and assigning a factor α for deflection of a centrally loaded rectangular plate which is based on a ratio of the plate geometry. The plate ratio b/a is 2.0, which gives a α factor of 0.01651. The D value can be calculated using the experimental results and the equation below [7]:

$$w_{max} = \alpha \frac{Pa^2}{D}$$

(1)

In Equation 1, $w_{max}$ is the max deflection at the center of the plate. P indicates the concentrated point load used, $\alpha$, is the short side of the rectangular plate. D represents the flexural rigidity term that shall be used to compare the stiffness's. Equation 1 was used by taking the experimental deflection values and the known concentrated load value and substituting to solve for the flexural rigidity term.

## 5.2 Governing Differential Equation
The fundamental assumptions of the small deflection theory of bending or so called classical or customary theory for isotropic, homogeneous, elastic, thin plates is based on geometry of deformations. The above assumptions, known as the Kirchoff hypothesis, are analogous to these associated with the simple bending theory of beams. The flexural rigidity of the plate is given by [4]:

$$D = \frac{Et^3}{12(1 - v^2)}$$

(2)

where D is the flexural rigidity, E is the modulus of Elasticity, h is the elastic thickness and $v$ is Poisson's ratio. The flexural rigidity $EI$ or bending stiffness is the quality that describes a filament's resistance to bending forces, just as stiffness describes a filament's resistance to elongation.

The governing differential equation of plate bending is [7]:

$$\frac{\partial^4 w}{\partial x^4} + 2\frac{\partial^4 w}{\partial x^2 \partial y^2} + \frac{\partial^4 w}{\partial y^4} = \frac{p}{D}$$

(3)

in which w is the deflection of the plate, p is an evenly distributed load on the plate, and D is given by Equation 2.

## 5.3 Boundary Conditions
The edges of the plate in the x and y axis are assumed to be taken parallel to the sides of the plate. A simply supported edge has a deflection at that edge as zero. At that same time that edge can rotate freely with respect to the edge line, which means that there are no moments alone the edge. Referring to Figure 5, the analytical expression for the boundary condition are [6]:

$$w = 0, \quad M_x = \frac{\partial^2 w}{\partial x^2} = 0 \quad from \ x = 0 \ to \ a$$

(4)

$$w = 0, \quad M_y = \frac{\partial^2 w}{\partial y^2} = 0 \quad from \ x = 0 \ to \ b$$

## 5.4 Finite-Difference Formulation
The analysis of the problem is based on a finite-difference solution of Equation 3 in which the following finite-difference equations were substituted back into the plate deflection equation. Then using the experimental deflections and known concentrated loads, the flexural rigidity term can be calculated.
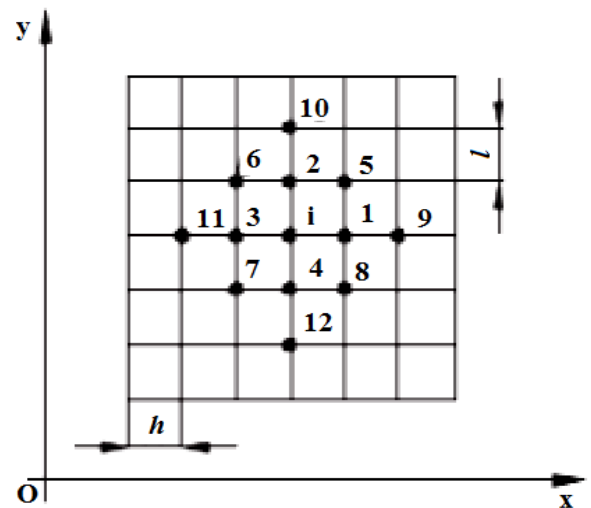


Fig. 6 - Generic Nodal Locations

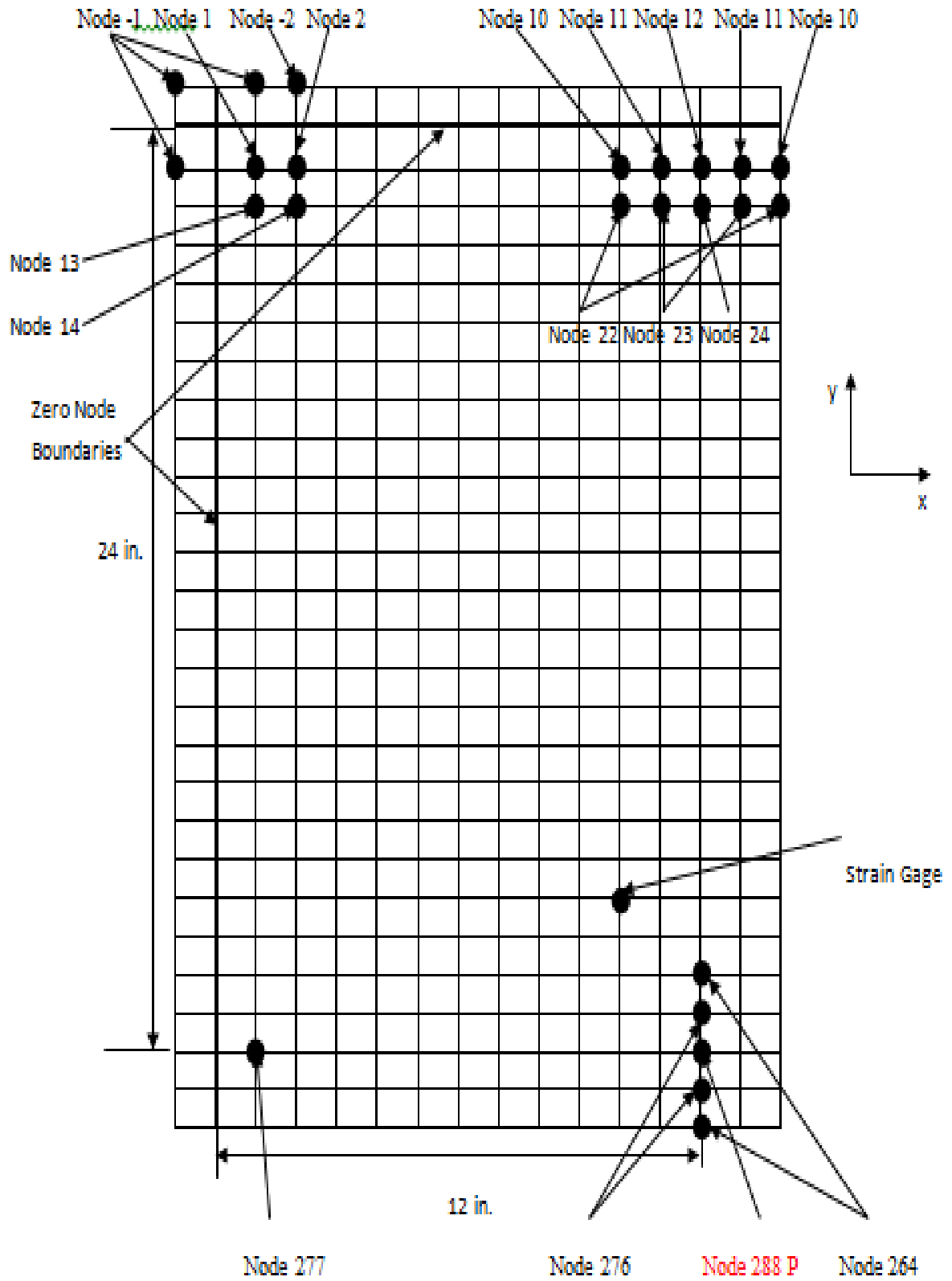Figure 6 shows the generic nodal locations for the finite-difference method. At the node $i$

Fig 7.  FRP – Deflection Nodal Diagram

with coordinates x and y, the first partial derivatives are given by [8]:

$$\left(\frac{\partial w}{\partial x}\right)_i = \frac{w_1 - w_3}{2h}$$

(5)

$$\left(\frac{\partial w}{\partial y}\right)_i = \frac{w_4 - w_2}{2l}$$

(6)

Similarly, the partial derivatives of the second, third and fourth orders are as follows [8]:

$$\left(\frac{\partial w^2}{\partial x^2}\right)_i = \frac{\partial}{\partial x}\left(\frac{\partial w}{\partial x}\right) = \frac{w_1 - 2w_i + w_3}{h^2}$$

(7)

$$\left(\frac{\partial w^2}{\partial y^2}\right)_i = \frac{\partial}{\partial y}\left(\frac{\partial w}{\partial y}\right) = \frac{w_2 - 2w_i + w_4}{l^2}$$

(8)

$$\left(\frac{\partial w^3}{\partial x^3}\right)_i = \frac{w_{10} - 2w_2 + 2w_4 - w_{12}}{2h^3}$$

(9)

$$\left(\frac{\partial w^3}{\partial y^3}\right)_i = \frac{w_{10} - 2w_2 + 2w_4 - w_{12}}{2l^3}$$

(10)

$$\left(\frac{\partial w^4}{\partial x^4}\right)_i = \frac{w_9 - 4w_1 + 6w_i + w_{11}}{h^4}$$

$$\left(\frac{\partial f^4}{\partial y^4}\right)_i = \frac{w_{10} - 4w_2 + 6w_i + w_{12}}{l^4}$$

(11)

Similarly [8]:

$$\left(\frac{\partial^2 w}{\partial x \, \partial y}\right)_i = \frac{\partial}{\partial y}\left(\frac{\partial w}{\partial x}\right) = \frac{w_6 - w_5 - w_7 + w_8}{l^2 h^2}$$

(12)

Substituting the above finite-difference equations into Equation 12, and setting $l = h$, results in [9]:

$$20\omega_i - 8(\omega_1 + \omega_2 + \omega_3 + \omega_4) + 2(\omega_5 + \omega_6 + \omega_7 + \omega_8) + \omega_9 + \omega_{10} + \omega_{11} + \omega_{12} = \frac{ph^4}{D}$$

(13)

To convert this point load to a distributed load, the point load is assumed to be distributed 2.54-cm by 2.54-cm. area over the node. The concentrated load is divided by the area [8]:

$$p = \frac{P}{lh}$$

(14)

Applying Equation 3 at each of the interior nodes of the plate, and incorporating the boundary conditions in the finite-difference form, a system of linear equations is first formulated in the following matrix form:

$$[K]\{\Delta\} = \{q\}$$

(15)

where [K] is the coefficient matrix, {Δ} is the unknown deflection vector, and {q} is the load vector. In this study, a total of 288 interior nodes were used, this means that equation 13 was applied at all the nodes, thus creating 288 simultaneous linear equations. Each one of these equations can be broken up into matrix notation, where all of the constants in the left side of each equation are then placed into the [K] matrix. The $\omega_i$ variables are placed in the {Δ} vector. The right side of each equation is placed in the {q} vector. Then solving for the {Δ} vector will result in the deflections for each node across the plate. For this problem the flexural rigidity term D was given a value based off the FRP plate known Young's Modulus and a measured thickness. These values where then used to determine D for the base FRP plate alone. As fabric was added to a plate the flexural rigidity value had to be matched to the experimental values recorded because no known Young's Modulus or equivalent thicknesses have been established for composite laminated materials.

Figure 7 shows the location of the nodes used in the finite-difference method. This is also a quarter of the actual plate. Node 1 starts at the top left corner and the numbers increase across the plate left
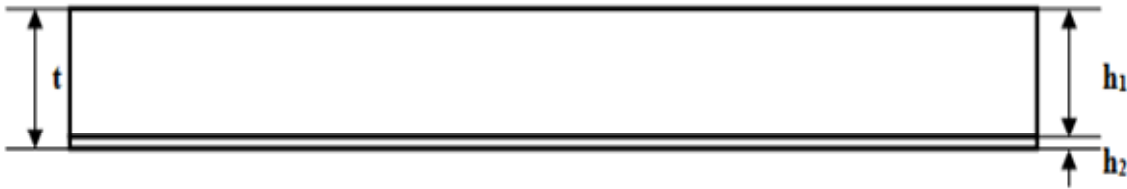
Fig 8. Cross Section Diagram of a Generic Plate

to right to node 12, the next row starts node 13 all the way down to the center point of the plate at node 288. This is also where the location of the point load is at the center of the plate. The strain gauges are on top and bottom, which are offset from the center four inches length wise and two inches width wise at node 238.

This is the nodal location system that was used in the finite-difference Matlab® program. Since the edges are simply supported there is a zero node around all of the edges. Also, a phantom point that extends beyond the plate is used to accurately compute the deflections. This point, due to the plate being simply supported, is equal in magnitude and opposite in direction to the point adjacent to the real plate side.

## 5.5 Thickness Flexural Rigidity Ratio

Figure 8 indicates the cross section of a plate, "t" is the total thickness of the plate, $h_1$ is the constant thickness of the FRP and $h_2$ is the variable thickness of the multiple fabrics. It also allows for the experimental results to be used in the theoretical calculations and to compute the Young's Modulus values for each of the plates.

$$t = h_1 + \frac{D}{D_o} h_2$$

(16)

In equation 16, $h_1$ is the constant thickness of the FRP plate which was 0.25 inches. The $D_o$ term is the flexural rigidity of the FRP plate with no fabric epoxied. D is the flexural rigidity term from a FRP plate and a fabric combination. This ratio of flexural rigidities allows for a ratio of the stiffness's to correlate into the fabric thickness $h_2$.

## 6 Problem Solution

Using the deflection results from the experiment, the computer program results can be matched by changing the flexural rigidity term as a whole. Once the computer deflection results match the experimental results, the flexural rigidity term has been found. This term then can be used to solve for the thickness and Young's Modulus by using equations 16 and 2 respectfully.

Table 1 summarizes the plate flexural rigidity (D), equivalent thickness (h), and Young's modulus (E) values for the baseline FRP plate as well as the retrofitted plates. In this table, the first column identifies the plate type. The second column list the D values calculated using the finite-difference method combined with experimental load-deflection relations. The third column presents the h values computed from Equation 2 using the experimental D values. The last column presents the respective E values also calculated by using Equation 2.

| Plate Type | Calculated Properties | | |
|---|---|---|---|
| | Flexural Rigidity (D) (MPa-cm³) | t (cm) | Young's Modulus (E MPa) |
| FRP only | 295.0 | 0.635 | $1.24 \times 10^4$ |
| FRP Retrofitted with Kevlar® | 351.0 | 0.653 | $1.36 \times 10^4$ |
| FRP Retrofitted with Carbon Fiber | 338.0 | 0.670 | $1.21 \times 10^4$ |
| FRP Retrofitted with Aerospace Grade Carbon Fiber | 488.0 | 0.753 | $1.23 \times 10^4$ |

Table 1 - Plate Flexural Rigidity and Young's modulus

Figure 9 represents a comparison of the experimental and theoretical load vs. deflection relations. The theoretical values of the slope of the load-deflection curve from this figure are 788.4 N/cm, 545.7 N/cm, and 567.6 N/cm, respectively, for the FRP plate with Aerospace Grade Carbon Fiber fabric, Carbon Fiber fabric, and Kevlar. The corresponding value for the baseline plate FRP plate is 476.5 N/cm.

The FRP plate has a maximum deflection-to-thickness ratio of 0.158. The FRP plate with Kevlar® fabric has a ratio of 0.125; the one with Carbon fiber fabric a ratio of 0.137; and that with the Aerospace Carbon fiber fabric a ratio of 0.092. The Aerospace Carbon fiber fabric increased the stiffness dramatically in comparison to the FRP. The Carbon fiber produced better results than Kevlar® experimentally.
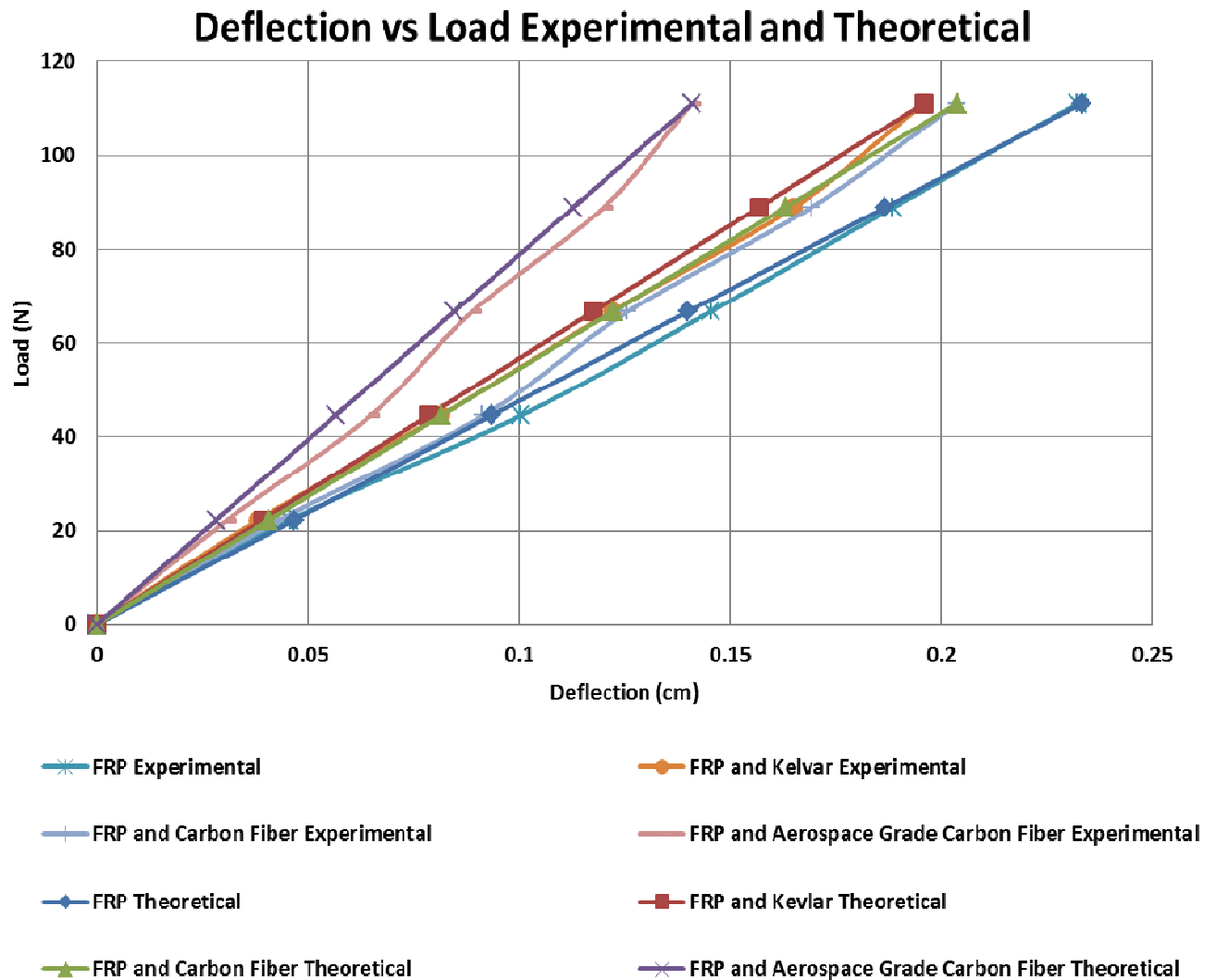


Fig 9. Deflection vs. Load comparing Experimental and Theoretical Results

# 7 Conclusion

The findings of this research are summarized as follows:

1) The epoxied fabrics increased the stiffness of the plates.

2) The Aerospace Grade Carbon fiber was the best retrofitting material to reduce the deflections and stresses.

3) After calculating the flexural rigidity values with the finite-difference method and taking the ratio between the control FRP plate and the plate coated with Kevlar®, the stiffness of the plate coated with Kevlar®, increased by 19 percent, the Carbon fiber plate stiffness increased by 15 percent and the Aerospace Grade Carbon fiber stiffness increased by 65 percent.

4) Comparing overall deflections, the Aerospace Grade Carbon fiber reduced the deflection the most, the Kevlar® was the next best and the Carbon fiber was the fabric that provided the least increase in stiffness.

5) The plate flexural rigidity values were validated with a direct comparison to Navier's flexural rigidity solution.

6) The finite-difference method together with experimental load-deflection relations can be used to accurately compute the plate flexural rigidity.

*References:*

[1] Du Pont. "Technical Guide Kevlar Aramid Fiber."*KevlarÂ® Aramid Fiber*. Du Pont. Web.11Apr.2012.http://www2.dupont.com/Kevlar/en_US/assets/downloads/KEVLAR_Technical_Guide.pdf>.

[2] Washer, Glenn. "Characterization of Kevlar Using Raman Spectroscopy. "*Characterization of Kevlar Using Raman Spectroscopy*. NASA.Web. <http://ntrs.nasa.gov/archive/nasa/casi.ntrs.nasa.gov/20070022474_2007020721.pdf>.

[3] Oghaleudolu. "HexForce Technical Fabrics Handbook."*Reinforcements for Composites*. Hexcel.Web. 11 Apr. 2012. <www.hexcel.com>.

[4] Daniel,, Isaac M., Jandro L. Abot,, Jyi-Jiin Luo1, and Patrick M. Schubel1. "Three-Dimensional Characterization of Constitutive Behavior and Failure of Textile Composites."Web.<http://www.icf11.com/proceeding/EXTENDED/5206.pdf>. 1Center for Intelligent Processing of Composites, Northwestern University, Evanston, IL 60208, USA 2Department of Aerospace Engineering and Engineering Mechanics, University of Cincinnati, Cincinnati, OH 45221, USA

[5] CREATIVE PULTRUSIONS, INC. "The Pultex Pultrusion Design Manual." *Imperical Design Manual*. CREATIVE PULTRUSIONS, INC.Web. <http://www.creativepultrusions.com/LitLibrary/designmanual/dmv4r6.pdf>. Imperial Version Volume 4 -Revisions 6

[6] Ventsel E., Krauthammer T. "Thin Plates and Shells-Theory, Analysis and Applications", Dekker NY. (2001), pp.200 – 225

[7] Timoshenko, Stephen, and S Woinowsky-Krieger. *Theory of Plates and Shells*. New York: McGraw-Hill, 1959.

[8] Dolic´anin, C´ B., V. B. Nikolic´, and D. C´ Dolic´anin."Application of Finite Difference Method to Study of the."SER. A: APPL. MATH. INFORM. AND MECH. 2.1(2010) (2010): 29+.

[9] Ketter, R. L., and S. P. Prawel, Jr. *Modern Methods of Engineering Computation*. New York: McGraw-Hill Book, 1969.

[10] Tarapada Roy AndDebabrataChakraborty. Delamination in Hybrid FRP Laminates under Low Velocity Impact Journal of Reinforced Plastics and Composites December 2006 25: 1939-1956

[11] Rahimi, Hamid, and Allan Hutchinson. "Concrete Beams Strengthened With Externally Bonded FRP Plates." Journal Of Composites For Construction 5.1 (2001): 44. Computers & Applied Sciences Complete. Web. 23 July 2012.

[12] Yen-Liang Yeh, Cheng Chi Wang, Ming-Jyi Jang, Using finite difference and differential transformation method to analyze of large deflections of orthotropic rectangular plate problem, Applied Mathematics and Computation, Volume 190, Issue 2, 15 July 2007, Pages 1146-1156

[13] Kyungsik Kim, Chai H. Yoo, Analytical solution to flexural responses of annular sector thin-plates, Thin-Walled Structures, Volume 48, Issue 12, December 2010, Pages 879-887